Signature splitting of the math xmlns="http://www.w3.org/1998/Math/MathML">msub>mi>g/mi>mrow>mn>7/mn>mo>//mo>mn>2/mn>/mrow>/msub>mrow>mo>[/mo>mn>404/mn>mo>]/mo>/mrow>msup>mrow>mn>7/mn>mo>//mo>mn>2/mn>/mrow>mo>+/mo>/msup>/math> bands in math xmlns="http://www.w3.org/1998/Math/MathML">mmultiscripts>mi>Ba/mi>mprescripts>/mprescripts>none>/none>mn>131/mn>/mmultiscripts>/math> and math xmlns="http://www.w3.org/1998/Math/MathML">mmultiscripts>mi>Ce/mi>mprescripts>/mprescripts>none>/none>mn>133/mn>/mmultiscripts>/math>

B. Ding et al.

Phys. Rev. C **104**, 064304 — Published 9 December 2021

DOI: 10.1103/PhysRevC.104.064304

Signature splitting of the $g_{7/2}[404]7/2^+$ bands in ^{131}Ba and ^{133}Ce

B. Ding,[1,2] C. M. Petrache,[3,*] S. Guo,[1,2,†] E. A. Lawrie,[4,5,‡] I. Wakudyanaye,[5,4] Z. H. Zhang,[6] H. L. Wang,[7] H. Y. Meng,[7] D. Mengoni,[8,9] Y. H. Qiang,[1,2] J. G. Wang,[1,2] C. Andreoiu,[10] A. Astier,[3] A. Avaa,[11,4] T. Bäck,[12] R. A. Bark,[4] D. Bazzacco,[8,9] A. Boso,[8,9] T. D. Bucher,[4,13] B. Cederwall,[12] M. V. Chisapi,[13,4] H. L. Fan,[1] F. Galtarossa,[14,15] F. H. Garcia,[10] A. Goasduff,[8,9] G. Jaworski,[14,16] P. Jones,[4] I. Kuti,[17] J. J. Lawrie,[4,5] G. S. Li,[1,2] R. Li,[1,3] M. L. Liu,[1,2] Z. Liu,[1,2] B. Lomberg,[5] B. F. Lv,[1,2] T. Marchlewski,[16] L. Mdletshe,[18,4] L. Msebi,[5,4] S. H. Mthembu,[5,4] D. R. Napoli,[14] A. Netshiya,[11,4] M. F. Nkalanga,[18,4] J. N. Orce,[5] K. Ortner,[10] F. Recchia,[8,9] S. Riccetto,[14] A. Rohilla,[1] T. W. Seakamela,[19,4] M. Siciliano,[14,20] M. A. Sithole,[5,4] D. Sohler,[17] J. Srebrny,[16] D. Testov,[8,9] A. Tucholski,[16] J. J. Valiente-Dobón,[14] F. Wentzel,[5] K. Whitmore,[10] Y. H. Zhang,[1,2] K. K. Zheng,[1,3] X. H. Zhou,[1,2] and B. R. Zikhali[5,4]

[1] *Key Laboratory of High Precision Nuclear Spectroscopy, Institute of Modern Physics, Chinese Academy of Sciences, Lanzhou 730000, People's Republic of China*
[2] *School of Nuclear Science and Technology, University of Chinese Academy of Science, Beijing 100049, People's Republic of China*
[3] *Universite Paris-Saclay, CNRS/IN2P3, IJCLab, 91405 Orsay, France*
[4] *iThemba LABS, National Research Foundation, PO Box 722, Somerset West 7129, South Africa*
[5] *Department of Physics, University of the Western Cape, Private Bag X17, 7535 Bellville, South Africa*
[6] *Mathematics and Physics Department, North China Electric Power University, Beijing 102206, China*
[7] *School of Physics and Microelectronics, Zhengzhou University, Zhengzhou 450001, China*
[8] *Dipartimento di Fisica e Astronomia, University degli Studi di Padova, I-35131 Padova, Italy*
[9] *INFN, Sezione di Padova, I-35131 Padova, Italy*
[10] *Department of Chemistry, Simon Fraser University, Burnaby, BC V5A 1S6, Canada*
[11] *School of Physics, University of Witwatersrand, Johannesburg, 2000, South Africa*
[12] *KTH Department of Physics, S-10691 Stockholm, Sweden*
[13] *Department of Physics, Stellenbosch University, P/B X1, Matieland 7602, South Africa*
[14] *INFN, Laboratori Nazionali di Legnaro, I-35020 Legnaro (Padova), Italy*
[15] *Dipartimento di Fisica e Scienze della Terra, University di Ferrara, Ferrara, Italy*
[16] *University of Warsaw, Heavy Ion Laboratory, Pasteura 5a, 02-093 Warsaw, Poland*
[17] *Institute for Nuclear Research, ATOMKI, 4001 Debrecen, Hungary*
[18] *University of Zululand, Department of Physics and Engineering, kwaDlangezwa, 3886, South Africa*
[19] *Department of Physics, University of Johannesburg, P.O. Box 524, Auckland Park 2006, South Africa*
[20] *Physics Department, Argonne National Laboratory, Lemont (IL), United States*

(Dated: November 9, 2021)

Excited states in ^{131}Ba and ^{133}Ce were studied using in-beam γ-ray spectroscopy through the ^{122}Sn(^{13}C,4n)^{131}Ba and ^{125}Te(^{12}C,4n)^{133}Ce reactions, respectively. A strongly-coupled band, associated with the $\nu g_{7/2}[404]7/2^+$ configuration, was identified in ^{131}Ba and ^{133}Ce. It is the first time to observe the $\nu g_{7/2}[404]7/2^+$ bands in the N=75 isotones. The signature partners exhibit considerable energy splitting in comparison with those in the $\pi g_{7/2}[404]7/2^+$ bands in the odd-A Ta and Re isotopes. Extensive cranked shell model and quasiparticle-plus-triaxial-rotor model calculations reveal the origin of the signature splitting, which depends not only on the triaxiality, but also on the configuration mixing with nearby low-j orbitals.

PACS numbers: 21.10.-k, 21.10.Re, 23.20.Lv, 27.60.+j

I. INTRODUCTION

The structure of an odd-A nuclear system can be described in the framework of the even-even core plus an odd number of quasiparticles. The interaction between the core and quasiparticles plays a key role in determining the excited nuclear spectra. According to the relative interaction strength, rotational bands in odd-A nuclei can be grouped as strongly-coupled, weakly-coupled, and decoupled bands in the frame of the particle-plus-rotor model [1, 2]. The strong coupling occurs if the Coriolis interaction is weak, which can be realized in the odd-A nuclei when the odd nucleon occupies a high-Ω Nilsson orbital. In particular, by coupling a quasiparticle occupying an $\Omega = j$ orbital to an axially deformed core, two cascades of $E2$ transitions merge into a single band composed of strong dipole and weak quadrupole crossover transitions.

Rotational bands associated with such configurations were widely observed in different mass regions of the nu-

* costel.petrache@ijclab.in2p3.fr
† gs@impcas.ac.cn
‡ elena@tlabs.ac.za

clear chart, for example the $\nu g_{9/2}[404]9/2^+$ bands in the $A \approx 100, 120$ mass regions [3–9], the $\nu h_{11/2}[505]11/2^-$ bands in the $A \approx 160$ mass region [10, 11], and the $\nu h_{9/2}[505]9/2^-$ bands in the $A \approx 180$ mass region [12, 13]. All these bands exhibit a signature splitting, defined as $S(I) = E(I) - E(I-1) - 1/2[E(I+1) - E(I) + E(I-1) - E(I-2)]$, almost equal to 0, as expected.

The signature splitting results from essentially the mixing of the $\Omega = 1/2$ orbital into the wave functions due to the Coriolis interaction. Such mixing is negligible for the high-j, $\Omega = j$ configurations in axially deformed nuclei. However, in triaxial deformed nuclei, the K quantum number is no longer conserved and the band configurations are a mixture of wave functions with different K values. Great efforts have been made to establish the relationship between triaxiality and the experimental observables. Meyer-Ter-Vehn investigated in detail the dependence on the triaxiality parameter γ of the particle-core coupling using particle-plus-triaxial-rotor model [14, 15]. More recently, one physical quantity that was proposed to quantify the degree of triaxiality is the signature splitting $S(I)$, which can be readily extracted from the level energies. It was explored in detail for the $\pi h_{11/2}[514]9/2^-$ bands in several neutron-rich rhenium isotopes, in which the increasing splitting amplitudes towards neutron-rich nuclei are monotonically proportional to the γ values deduced from the particle-rotor model [16].

It is interesting to further investigate the impact of the triaxiality on the signature splitting of the strongly coupled $\Omega = j$ bands in other nuclei, like the $N = 75$ isotones in the $A \approx$130 region, which are built on configurations with significant triaxiality [17–22]. The low-lying yrast states in ^{131}Ba and ^{133}Ce can be only reproduced by assuming large γ deformations ($\gamma \sim -20°$) [23, 24]. In addition, multiple chiral doublet bands were observed in ^{131}Ba [25] and ^{133}Ce [26], indicating triaxial shapes for both nuclei. With $N = 75$, the $\nu g_{7/2}[404]7/2^+$ orbital comes close to the Fermi surface, making it possible to study the dependence of the signature splitting on the triaxiality.

Prior to this work, low-spin states in ^{131}Ba were observed from electron capture (EC) and isomeric decay studies [27–29], as well as from transfer reaction studies [30, 31]. Later, high-spin states up to $43/2^-$ and $39/2^+$ were identified through heavy-ion induced reactions [23, 25, 32, 33]. The ^{133}Ce nucleus was also studied previously via an electron capture decay [34] and in-beam γ spectroscopy by employing various combinations of heavy-ion beams and targets [24, 26, 35–41]. In this work, we report the newly observed $\nu g_{7/2}[404]7/2^+$ bands in ^{131}Ba and ^{133}Ce and study the dependence of the signature splitting on the γ deformation parameter using configuration-constrained potential energy surface (PES) calculations [42–44] and quasiparticle-plus-triaxial-rotor (QTR) model [45].

II. EXPERIMENT AND RESULTS

A. Measurements

Excited states in ^{131}Ba were populated via the fusion-evaporation ^{122}Sn(^{13}C,4n)^{131}Ba reaction. The ^{13}C beam, with an energy of 65 MeV and intensity of 5 pnA, was provided by the XTU Tandem accelerator at the Laboratori Nazionali di Legnaro. The target was a stack of two self-supporting ^{122}Sn foils each with a thickness of 0.5 mg/cm^2. Prompt γ rays were detected by the GALILEO spectrometer [55] consisting of 25 Compton suppressed high-purity germanium (HPGe) detectors, placed in four rings at 90° (10 detectors), 119° (5 detectors), 129°(5 detectors), and 152° (5 detectors). To distinguish different reaction channels, charged particles and neutrons were detected by the EUCLIDES silicon ball [56] and the Neutron Wall array, respectively [57, 58]. Data were recorded by the GALILEO data acquisition system [59]; a total of 1.2×10^9 triple- or higher-fold events were collected. After Doppler correction of the γ energies, the $\gamma\gamma\gamma$ coincidence events were sorted into a three-dimensional histogram (cube) and the analysis was carried out with the RADWARE [60] and GASPware [61] software packages. A two-point angular-correlation ratio, R_{ac} [62], using the detectors placed at 90° and 152°, was employed to deduce the transition multipolarities. R_{ac} is independent of the multipolarity of the gating transition, and it was established to be ≈ 1.54 for stretched-quadruple and ≈ 0.77 for stretched-dipole transitions as in Ref. [25]. More details of the experiment and the data analysis were described in Refs. [25, 63, 64].

The second experiment was performed at the separated sector cyclotron of iThemba LABS near Cape Town, South Africa. High-spin states in ^{133}Ce were populated via the ^{125}Te(^{12}C,4n)^{133}Ce reaction at a beam energy of 57 MeV and an intensity of 5 pnA. The target was an isotopically enriched (95.3%) ^{125}Te metallic foil with a thickness of 2 mg/cm^2 on an 8 mg/cm^2 gold backing. The γ rays emitted by the excited residual nuclei were measured with the AFRODITE array [65, 66] consisting of eight Compton-suppressed clover detectors arranged in two rings at 90° (four clovers) and 135° (four clovers) with respect to the beam direction. 2.8×10^{10} double- and 5.4×10^9 triple- and higher-fold coincidence events were collected and sorted into two- and three-dimensional matrices for offline analysis. Data analysis was similar to that of ^{131}Ba as mentioned above. Typical R_{ac} ratios were $\approx$ 1.27 for stretched-quadrupole and $\approx$ 0.74 for stretched-dipole transitions, which were deduced from the known stretched quadrupole and dipole transitions in nuclei populated in the reaction.

B. Level schemes

The partial level schemes of ^{131}Ba and ^{133}Ce deduced from the present work are shown in Fig. 1. The level

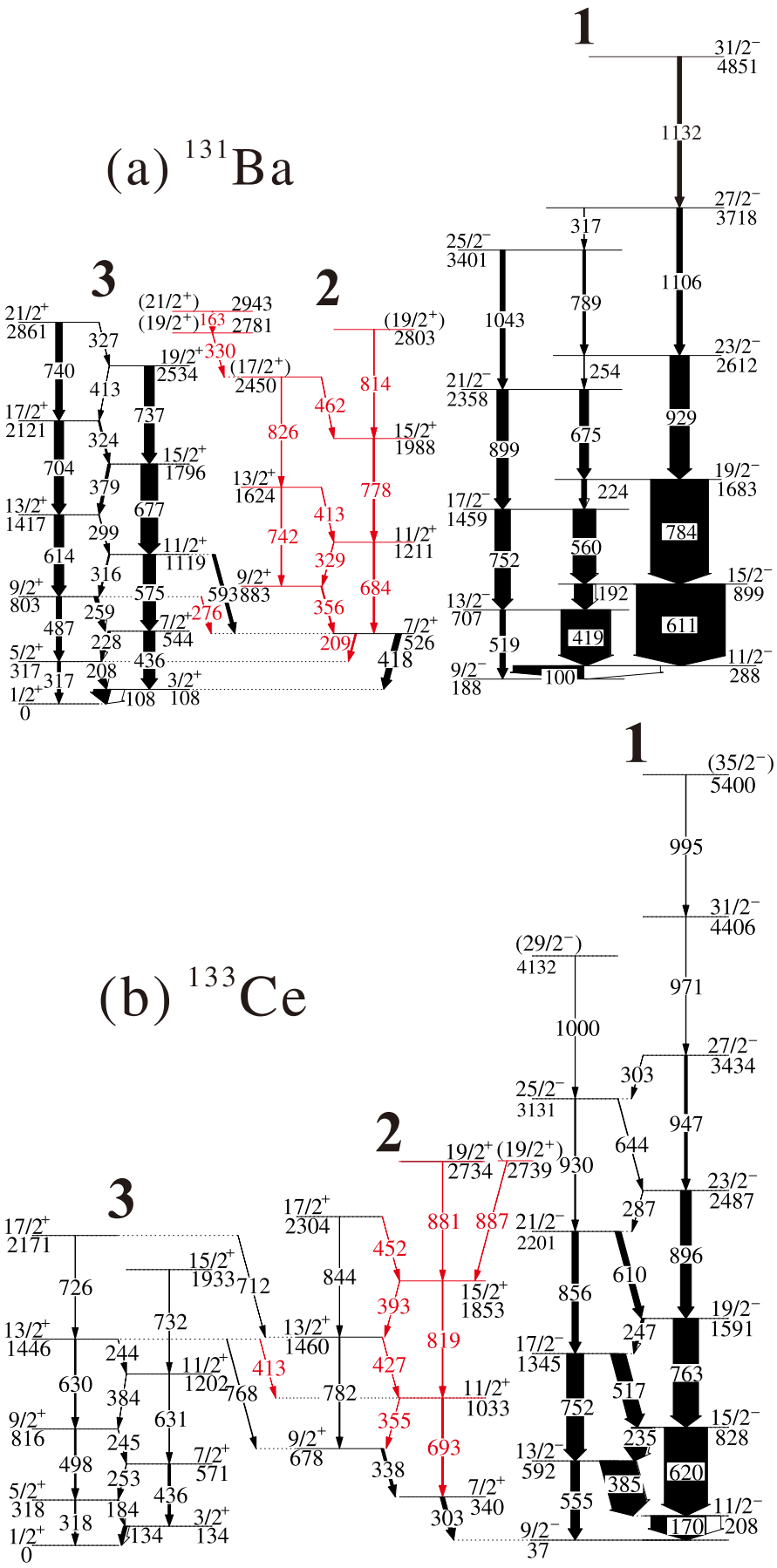

FIG. 1. Partial level schemes of ^{131}Ba and ^{133}Ce deduced from the present work. Newly observed transitions are marked in red.

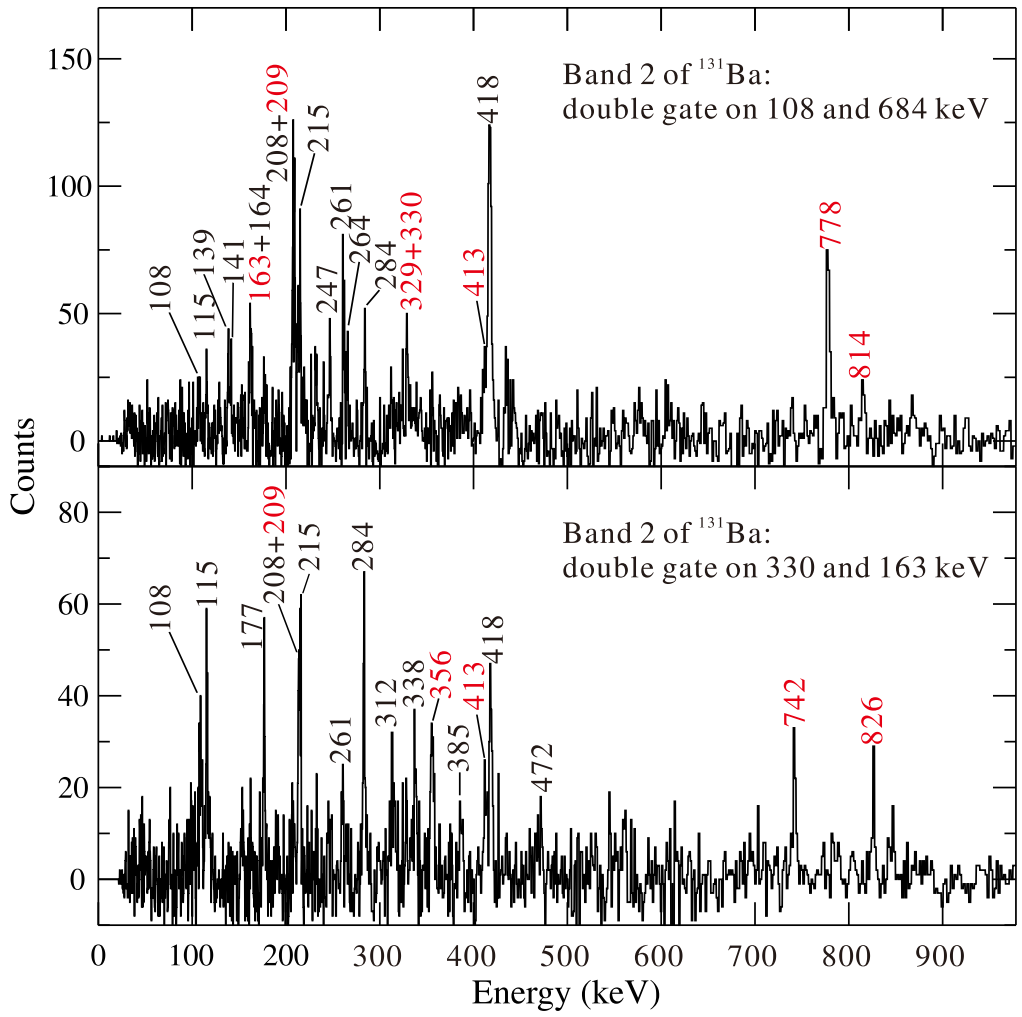

FIG. 2. Typical double-gated coincidence spectra for the new structures in ^{131}Ba. Newly observed levels are marked in red.

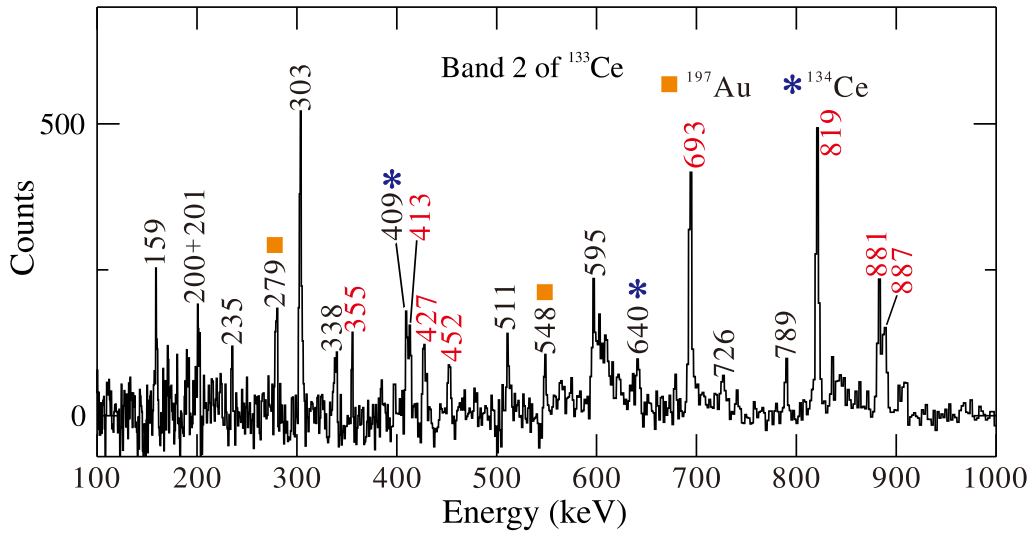

FIG. 3. Similar to Fig. 2, but for ^{133}Ce. The spectrum is obtained by summing the double-gated spectra on all combinations of the 303, 693, and 819-keV transitions.

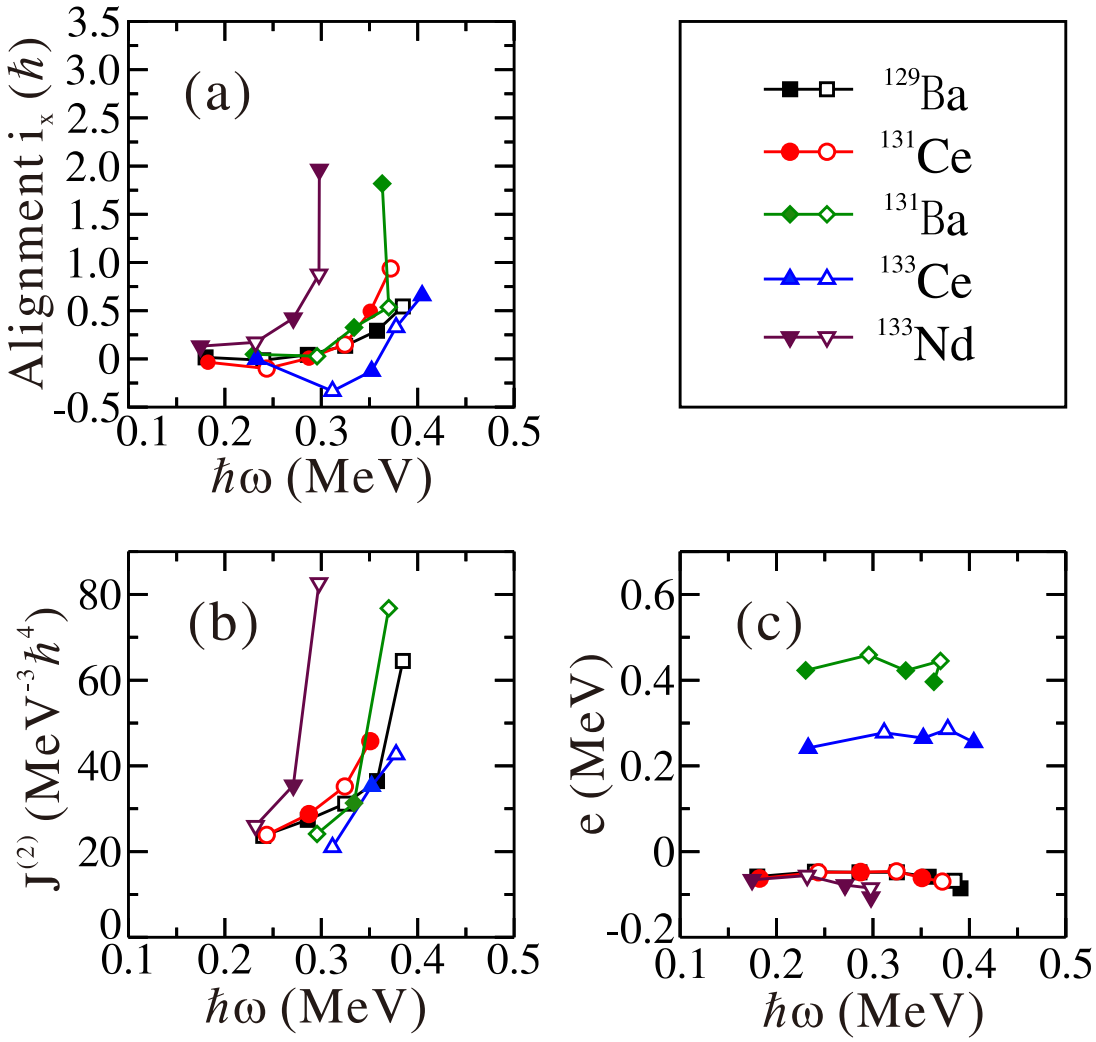

FIG. 4. (a) Experimental quasiparticle alignments (i_x), (b) dynamical moments of inertia $J^{(2)}$, and (c) quasi-neutron Routhian energies (e) of the $\nu g_{7/2}$ bands in $N = 75$ isotopnes ^{131}Ba, ^{133}Ce, as well as in $N = 73$ isotones ^{129}Ba, ^{131}Ce, and ^{133}Nd. The data for ^{131}Ba and ^{133}Ce are from this work, and the others are taken from [46] for ^{129}Ba, [47] for ^{131}Ce, and [48] for ^{133}Nd.

scheme for each nucleus consists of three rotational bands labeled as 1, 2, and 3, among which band 2 is newly identified. Typical double-gated spectra are shown in Figs. 2 and 3. In ^{131}Ba, band 2 is built on the 526-keV state which was first observed from an EC-decay measurements [28]. The spin-parity $I^\pi = 7/2^+$ was assigned to this state based on the quadrupole character of the 418-keV transition decaying to the $I^\pi = 3/2^+$ state of band 3 [23]. The existence of the 418-keV transition and its quadrupole nature are confirmed in this work. The branch with positive signature ($\alpha = +1/2$) of band 2 is connected with the higher-lying three-quasiparticle bands (i.e., bands D5 and D3 in Fig. 1 of Ref. [25]) via the cascade of the 163- and 330-keV transitions. The 826- and 742-keV transitions, together with the transitions from band D5 (D3), such as the 177- and 312-keV (215-, 284-, 338-, 385-, and 472-keV) transitions, are evident in the spectrum gated by the 163- and 330-keV linking cascade presented in the lower panel in Fig. 2. This supports the assignment of the 826- and 742-keV transitions to ^{131}Ba. The 330-keV transition is found to be a doublet: one component in the doublet is the linking transition mentioned above, and the other one (329 keV) is assigned as the transition feeding the $9/2^+$ state in band 2.

In ^{133}Ce, the 844- and 782-keV sequence in band 2 was reported recently (band Q1 in Fig. 1 of Ref. [26]); this sequence was found to feed the 340-keV $7/2^+$ state via a dipole transition of 338 keV. From the detailed analysis of the present data, we identified a new branch consisting of the 881-, 819-, and 693-keV transitions as it is shown in Fig. 3. The observation of the 413-keV transitions between band 2 and 3 supports the existence of the level at 1033 keV and thus the newly established branch of Band 2. Together with the previously known sequence, it concurs to the formation of band 2 of ^{133}Ce. The con-

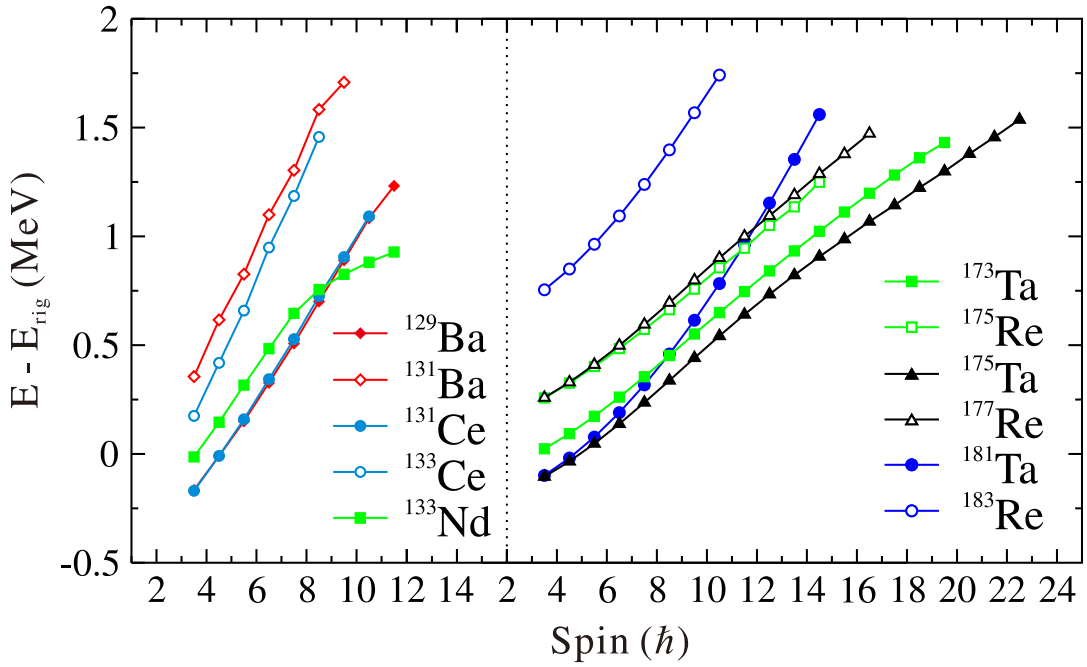

FIG. 5. The experimental excitation energies of the $\pi g_{7/2}$ bands in Re and Ta isotopes, and the $\nu g_{7/2}$ bands in Ba and Ce isotopes. An average liquid-drop energy $E_{\rm rig} = (\hbar^2/2\mathcal{J}_{\rm rig})I(1+1)$, where $\mathcal{J}_{\rm rig}$ =2/5AMR^2, was subtracted. The data on ^{131}Ba and ^{133}Ce are from this work, while those on the other isotopes are from the following references: ^{129}Ba [46], ^{131}Ce [47], ^{133}Nd [48], ^{175}Re [49], ^{177}Re [50], ^{183}Re [51], ^{173}Ta [52], ^{175}Ta [53], and ^{181}Ta [54].

nections between the two branches of 338, 355, 427, and 452 keV are also observed. The measured spectroscopic data (γ-ray energies, relative intensities, R_{ac} ratios, and suggested spin and parity assignments) are summarized in Table I and II for ^{131}Ba and ^{133}Ce, respectively.

III. DISCUSSION

A. Band properties and configuration assignments

The bands shown in Fig. 1 correspond to one-quasiparticle configurations. Band 1 was already reported previously and assigned to the $\nu h_{11/2}[514]9/2^-$ configuration in both ^{131}Ba and ^{133}Ce [23, 24, 26]. Band 3 is the ground state band; the $\nu s_{1/2}[400]1/2^+$ configuration with a possible admixture of the $\nu d_{3/2}[402]3/2^+$ configuration was suggested for such bands [23, 24, 36]. Bands 2 in the two nuclei based on the $I^\pi = 7/2^+$ state are newly identified in the present work. They have strongly coupled character, exhibiting intense in-band $M1 + E2$ transitions, indicating high-K configurations. From the inspection of the available intrinsic Nilsson orbitals near the Fermi surface for $N = 75$, one can realize that only the $\nu g_{7/2}[404]7/2^+$ configuration is in agreement with such band properties. Bands built on the $\nu g_{7/2}[404]7/2^+$ orbital were already observed in the $N = 73$ isotones ^{129}Ba, ^{131}Ce, and ^{133}Nd, and they were strongest populated among the positive-parity bands in all three nuclei. Thus, it is natural to expect the existence of similar bands in the neighboring $N = 75$ isotones. Additionally, the $7/2^+$ band-head energies were calculated to lie at energies which differ by about 30 and 100 keV (see Table III) with respect to the experimental energies in ^{133}Ce and ^{131}Ba, respectively, supporting the $\nu g_{7/2}[404]7/2^+$ assignment for bands 2. It is noted that the $I^\pi = 7/2^+$ band head in ^{131}Ba is fully depopulated to band 3 via the $M1+E2$ 209- and the $E2$ 418-keV transitions. This can be attributed to the configuration mixing of the $7/2^+$ states in the two bands, since the two $7/2^+$ states are located very close to each other with excitation energies differing by only 18 keV. A similar situation occurs for the $13/2^+$ states in bands 2 and 3 of ^{133}Ce. For the $I^\pi = 7/2^+$ band head in ^{133}Ce, the configuration mixing is expected to be less because the energy spacing between the $7/2^+$ states of bands 2 and 3 is larger. As a consequence of this lower mixing, the depopulation of band 2 proceeds through the $E1$ 303-keV transition to band 1.

A comparison between the $\nu g_{7/2}[404]7/2^+$ bands in ^{129,131}Ba, ^{131,133}Ce, and ^{133}Nd is shown in Fig. 4. The standard plots of the quasiparticle-aligned angular momenta (i_x) and the dynamical moments of inertia ($J^{(2)}$) as functions of the rotational frequency ($\hbar\omega$) are shown in Fig. 4 (a) and 4 (b), respectively. The used Harris parameters are $\mathcal{J}_0 = 13.4\ \hbar^2$MeV^{-1} and $\mathcal{J}_1 = 33.2\ \hbar^4$MeV^{-3} for ^{131}Ba and ^{133}Ce as in Ref. [24], and $\mathcal{J}_0 = 18.6\ \hbar^2$MeV^{-1} and $\mathcal{J}_1 = 29.1\ \hbar^4$MeV^{-3} for ^{129}Ba,

TABLE I. Energies of initial states, transition energies, relative γ-ray intensities, angular correlation ratios ($R_{\rm ac}$), multipolarities, and spin and parity assignments in ^{131}Ba. Transitions are grouped in bands by their initial states.

$E_{\rm i}$(level)	E_γ(keV)[a]	I_γ	$R_{\rm ac}$ ratio	Mult.	$I_{\rm i}^\pi \rightarrow I_{\rm f}^\pi$
Band 1					
288.0	100.0	100(8)	0.67(6)	M1+E2	$11/2^- \rightarrow 9/2^-$
706.7	418.7	69(6)	0.29(3)	M1+E2	$13/2^- \rightarrow 11/2^-$
	518.7	7.5(8)	1.6(2)	E2	$13/2^- \rightarrow 9/2^-$
899.2	192.4	26(3)	0.54(6)	M1+E2	$15/2^- \rightarrow 13/2^-$
	611.2	125(15)	1.5(1)	E2	$15/2^- \rightarrow 11/2^-$
1459.0	559.9	32(3)	0.30(4)	M1+E2	$17/2^- \rightarrow 15/2^-$
	752.3	22(2)	1.7(3)	E2	$17/2^- \rightarrow 13/2^-$
1683.3	224.3	6.4(7)	0.61(5)	M1+E2	$19/2^- \rightarrow 17/2^-$
	784.1	81(7)	1.5(1)	E2	$19/2^- \rightarrow 15/2^-$
2357.9	674.6	12(2)	0.22(6)	M1+E2	$21/2^- \rightarrow 19/2^-$
	898.9	16(2)	1.5(2)	E2	$21/2^- \rightarrow 17/2^-$
2611.9	253.9	$\leq$1		(M1+E2)	$23/2^- \rightarrow 21/2^-$
	928.6	27(2)	1.6(1)	E2	$23/2^- \rightarrow 19/2^-$
3401.1	789.3	3.7(5)	0.8(6)	M1+E2	$25/2^- \rightarrow 23/2^-$
	1043.2	5.6(9)	1.5(2)	E2	$25/2^- \rightarrow 21/2^-$
3718.2	317.0	$\leq$1		(M1+E2)	$27/2^- \rightarrow 25/2^-$
	1106.3	7.7(8)	1.6(2)	E2	$27/2^- \rightarrow 23/2^-$
4850.6	1132.4	1.9(6)	1.5(2)	E2	$31/2^- \rightarrow 27/2^-$
Band 2					
526.3	417.9	8(1)	1.5(3)	E2	$7/2^+ \rightarrow 3/2^+$
	209.4	1.8(6)		(M1+E2)	$7/2^+ \rightarrow 5/2^+$
882.5	356.2	1.5(5)	0.8(1)	M1+E2	$9/2^+ \rightarrow 7/2^+$
1210.7	328.7	$\leq$1		(M1+E2)	$11/2^+ \rightarrow 9/2^+$
	684.4	2.1(8)	1.3(5)	E2	$11/2^+ \rightarrow 7/2^+$
1624.1	412.5	$\leq$1		(M1+E2)	$13/2^+ \rightarrow 11/2^+$
	741.6	1.1(4)	1.6(4)	E2	$13/2^+ \rightarrow 9/2^+$
1988.4	777.7	1.8(7)	1.5(4)	E2	$15/2^+ \rightarrow 11/2^+$
2450.2	461.8	$\leq$1		(M1+E2)	$(17/2^+) \rightarrow 15/2^+$
	826.1	$\leq$1		(E2)	$(17/2^+) \rightarrow 13/2^+$
2802.8	814.4	$\leq$1		(E2)	$(19/2^+) \rightarrow 15/2^+$
2780.5	330.3	$\leq$1		(M1+E2)	$(19/2^+) \rightarrow (17/2^+)$
2943.2	162.7	$\leq$1		(M1+E2)	$(21/2^+) \rightarrow (19/2^+)$
Band 3					
108.4	108.4	23(2)	0.9(1)	M1+E2	$3/2^+ \rightarrow 1/2^+$
316.8	208.3	11(3)	0.8(1)	M1+E2	$5/2^+ \rightarrow 3/2^+$
	316.8	5(2)	1.1(2)	E2	$5/2^+ \rightarrow 1/2^+$
544.2	227.5	4(2)	0.7(1)	M1+E2	$7/2^+ \rightarrow 5/2^+$
	435.8	16(2)	1.2(1)	E2	$7/2^+ \rightarrow 3/2^+$
803.3	259.1	4(2)		(M1+E2)	$9/2^+ \rightarrow 7/2^+$
	486.5	10(2)	1.3(1)	E2	$9/2^+ \rightarrow 5/2^+$
	276.1	$\leq$1		(M1+E2)	$9/2^+ \rightarrow 7/2^+$
1118.9	315.5	1.6(6)		(M1+E2)	$11/2^+ \rightarrow 9/2^+$
	574.7	15(2)	1.4(1)	E2	$11/2^+ \rightarrow 7/2^+$
	593.0	4(2)	1.5(2)	E2	$11/2^+ \rightarrow 7/2^+$
1417.0	298.5	1.1(4)		(M1+E2)	$13/2^+ \rightarrow 11/2^+$
	613.7	12(2)	1.6(2)	E2	$13/2^+ \rightarrow 9/2^+$
1796.3	379.2	3(1)	0.6(1)	M1+E2	$15/2^+ \rightarrow 13/2^+$
	677.4	19(3)	1.5(2)	E2	$15/2^+ \rightarrow 11/2^+$
2120.8	324.0	3(1)		(M1+E2)	$17/2^+ \rightarrow 15/2^+$
	703.8	10(2)	1.4(1)	E2	$17/2^+ \rightarrow 13/2^+$
2533.7	412.5	$\leq$1		(M1+E2)	$19/2^+ \rightarrow 17/2^+$
	737.4	12(2)	1.4(2)	E2	$19/2^+ \rightarrow 15/2^+$
2861.1	327.0	$\leq$1		(M1+E2)	$21/2^+ \rightarrow 19/2^+$
	740.3	2.5(9)	1.4(2)	E2	$21/2^+ \rightarrow 17/2^+$

[a] The γ-ray energies are estimated to be accurate to $\pm$0.3 keV for the strong transitions ($I_\gamma > 10$), rising to $\pm$0.7 keV for the weaker transitions.

TABLE II. Similar to table I, but for ^{133}Ce.

$E_{\rm i}$(level)	E_γ(keV)[a]	I_γ	$R_{\rm ac}$ ratio	Mult.	$I_{\rm i}^\pi \to I_{\rm f}^\pi$
Band 1					
207.5	170.3	100(6)	0.8(1)	M1+E2	$11/2^- \to 9/2^-$
592.4	384.9	63(5)	0.59(6)	M1+E2	$13/2^- \to 11/2^-$
	555.1	16(2)	1.3(1)	E2	$13/2^- \to 9/2^-$
827.5	235.1	37(3)	0.75(8)	M1+E2	$15/2^- \to 13/2^-$
	620.0	78(8)	1.3(2)	E2	$15/2^- \to 11/2^-$
1344.5	517.0	26(11)	0.58(6)	M1+E2	$17/2^- \to 15/2^-$
	752.0	31(3)	1.3(2)	E2	$17/2^- \to 13/2^-$
1590.9	246.6	4.7(5)	0.8(1)	M1+E2	$19/2^- \to 17/2^-$
	763.4	46(4)	1.4(2)	E2	$19/2^- \to 15/2^-$
2200.9	610.0	11(2)	0.7(1)	M1+E2	$21/2^- \to 19/2^-$
	856.4	11(1)	1.3(1)	E2	$21/2^- \to 17/2^-$
2487.3	286.6	0.3(1)	0.8(1)	M1+E2	$23/2^- \to 21/2^-$
	896.4	20(2)	1.2(1)	E2	$23/2^- \to 19/2^-$
3131.2	643.6	0.9(2)	0.6(1)	M1+E2	$25/2^- \to 23/2^-$
	930.3	1.9(3)	1.3(1)	E2	$25/2^- \to 21/2^-$
3434.3	303.0	0.2(1)		(M1+E2)	$27/2^- \to 25/2^-$
	947.0	5.0(5)	1.3(2)	E2	$27/2^- \to 23/2^-$
4131.5	1000.3	0.5(2)	1.0(2)	(E2)	$(29/2^-) \to 25/2^-$
4405.6	971.3	0.6(2)	1.5(2)	E2	$31/2^- \to 27/2^-$
5400.1	994.5	≤ 0.6		(E2)	$(35/2^-) \to 31/2^-$
Band 2					
340.3	303.1	7.5(9)	1.0(1)	E1	$7/2^+ \to 9/2^-$
678.4	338.1	4.7(5)	0.6(1)	M1+E2	$9/2^+ \to 7/2^+$
1033.1	354.8	0.4(1)	0.7(1)	M1+E2	$11/2^+ \to 9/2^+$
	692.8	2.8(6)	1.3(2)	E2	$11/2^+ \to 7/2^+$
1459.9	426.6	0.2(1)	0.8(2)	M1+E2	$13/2^+ \to 11/2^+$
	781.5	1.6(4)	1.3(2)	E2	$13/2^+ \to 9/2^+$
1852.5	392.5	0.1(1)		(M1+E2)	$15/2^+ \to 13/2^+$
	819.4	1.5(4)	1.2(1)	E2	$15/2^+ \to 11/2^+$
2304.3	451.7	0.1(1)	0.7(2)	M1+E2	$17/2^+ \to 15/2^+$
	844.4	0.5(3)	1.2(2)	E2	$17/2^+ \to 13/2^+$
2733.9	881.4	0.4(2)	1.4(3)	E2	$19/2^+ \to 15/2^+$
2739.3	886.8	≤ 0.4		(E2)	$(19/2^+) \to 15/2^+$
Band 3					
134.3	134.3	7.1(5)	1.0(1)	M1+E2	$3/2^+ \to 1/2^+$
318.1	183.8	2.8(2)	0.8(1)	M1+E2	$5/2^+ \to 3/2^+$
	318.0	2.0(2)	1.3(2)	E2	$5/2^+ \to 1/2^+$
570.7	252.7	0.8(2)	0.9(1)	M1+E2	$7/2^+ \to 5/2^+$
	436.4	4.3(3)	1.2(2)	E2	$7/2^+ \to 3/2^+$
815.7	244.9	0.5(2)		(M1+E2)	$9/2^+ \to 7/2^+$
	497.6	2.8(3)	1.4(2)	E2	$9/2^+ \to 5/2^+$
1201.6	384.4	0.2(1)		(M1+E2)	$11/2^+ \to 9/2^+$
	630.9	0.9(5)	1.3(2)	E2	$11/2^+ \to 7/2^+$
1445.7	244.4	0.2(1)		(M1+E2)	$13/2^+ \to 11/2^+$
	630.0	3(2)	1.2(3)	E2	$13/2^+ \to 9/2^+$
	412.5	0.2(1)	0.6(2)	M1+E2	$13/2^+ \to 11/2^+$
	767.5	1.0(3)	1.2(3)	E2	$13/2^+ \to 9/2^+$
1933.4	731.8	0.3(1)	1.4(6)	E2	$15/2^+ \to 11/2^+$
2171.4	725.7	0.7(2)	1.4(2)	E2	$17/2^+ \to 13/2^+$
	711.6	0.3(1)	1.4(3)	E2	$17/2^+ \to 13/2^+$

[a] The γ-ray energies are estimated to be accurate to ± 0.3 keV for the strong transitions ($I_\gamma > 10$), rising to ± 0.8 keV for the weaker transitions.

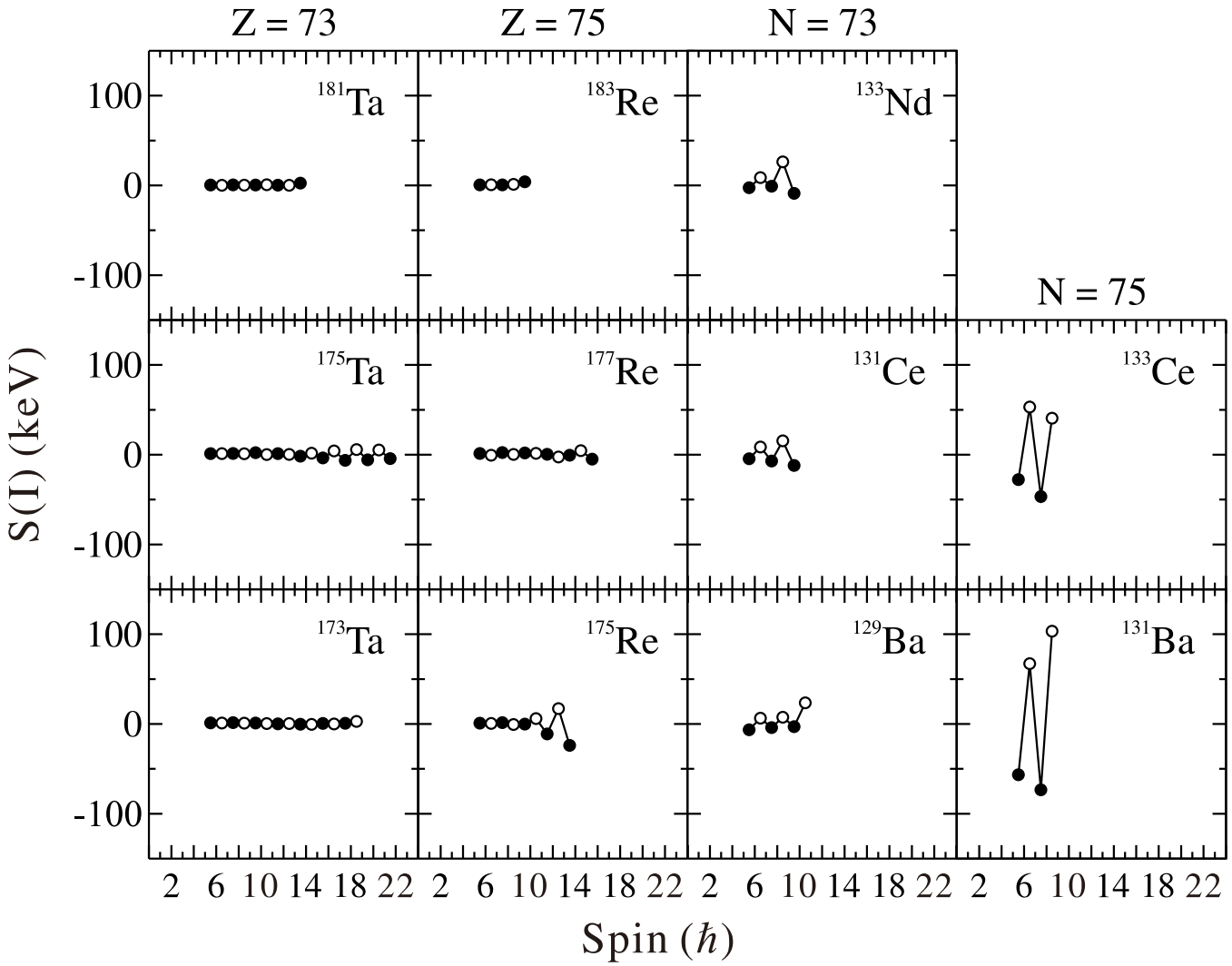

FIG. 6. Signature splittings of the $\pi g_{7/2}$ and $\nu g_{7/2}$ bands in the $Z = 73, 75$ isotopes and $N = 73, 75$ isotones. The data are the same to Fig. 5.

^{131}Ce, and ^{133}Nd, which were obtained by fitting the yrast band of ^{129}Ba [46]. The initial alignment i_x and $J^{(2)}$ of these bands before the first up-bending are similar, being consistent with the same configuration assignment. The angular momentum of the $[404]7/2^+$ band was extended up to a high-spin region in $N = 73$ isotones ($55/2\hbar$ in ^{129}Ba, $51/2\hbar$ in ^{131}Ce, and $67/2\hbar$ in ^{133}Nd), while only medium-spin states were observed in $N = 75$ isotones (maximum $19/2^+$). This can be attributed to the increasing excitation energies of the quasiparticle states, as can be seen in Fig. 4 (c) which shows the experimental quasi-neutron Routhians e of the bands in the five nuclei.

B. Signature splittings in the proton and neutron $g_{7/2}[404]\mathbf{7/2^+}$ bands

The $[404]7/2^+$ bands originating from either valence neutron or proton excitations can also be compared to get a further insight into the band properties. The $\pi g_{7/2}[404]7/2^+$ bands were widely reported in the odd-even Ta isotopes with mass number A ranging from 167 to 185; the $I^\pi = 7/2^+$ band head appears to be the ground state in $^{175-185}$Ta [52–54, 67–73]. Such bands were also observed in ^{175}Re [49], ^{177}Re [50], and ^{183}Re [51]. The observations were qualitatively attributed to the large quadrupole deformation [49] or the crossing with a highly aligned band [51]. In the odd-A Ir isotopes no $[404]7/2^+$ band was observed in the whole isotopic chain. The excitation energies and signature splittings $S(I)$ of both $\pi g_{7/2}[404]7/2^+$ and $\nu g_{7/2}[404]7/2^+$ bands are systematically compared in Figs. 5 and 6. It

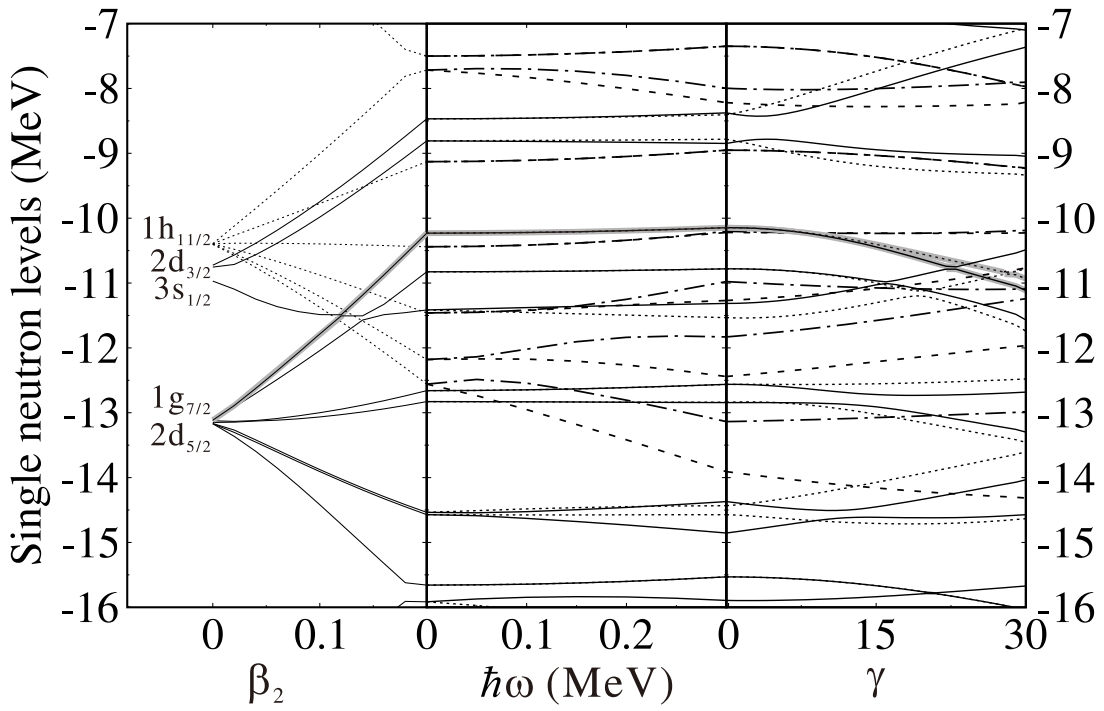

FIG. 7. Calculated quasineutron Routhians as a function of quadrupole deformation (β_2), rotational frequency ($\hbar\omega$), and triaxiality (γ). The parity and signature (π, α) of the Routhians are represented as follows: (+, +1/2) solid lines, (+, -1/2) dotted lines, (-, +1/2) dash-dotted lines, and (-, -1/2) dashed lines. Two signature branches of the $\nu g_{7/2}[404]7/2^+$ orbital are shown on a shade background.

is worth noting that the $7/2^+$ ($13/2^+$) states in bands 2 (3) of ^{131}Ba (^{133}Ce) are close in energy. Generally speaking, the interaction between the $s_{1/2}$ and $g_{7/2}$ bands can lead to the mixing of the wave functions and extra energy shifts on the corresponding levels, which can also contribute to the observed signature splitting amplitude. Nevertheless, the possible interaction strength between the involved states is less than half of the energy spacing between the corresponding states, that is 9 (7) keV in ^{131}Ba (^{133}Ce), which would correspond to degenerate states before the interaction. Therefore, taking into account the mixing between the nearly degenerate $7/2^+$ ($13/2^+$) states in bands 2 (3) in ^{131}Ba (^{133}Ce) would only induce negligible contributions.

The excitation energies of the corresponding states in $N, Z = 73$ nuclei are lower relative to those in the $N, Z = 75$ ones. An energy gap can be clearly seen in Fig. 5 between $N = 73$ and $N = 75$ for both Ba and Ce isotopes, with a larger gap in the Ba isotopes. It corresponds to the $N = 74$ gap between the $\nu g_{7/2}[404]7/2^+$ and $\nu h_{11/2}[514]9/2^-$ orbitals in the Nilsson diagram, implying that the former orbital is closer to the Fermi surface and thus the configuration involving the 73$^{\rm rd}$ valence neutron is less excited than that involving the 75$^{\rm th}$ one. This gives a qualitative explanation of the experimental facts that higher population intensities and higher-spin states were systematically observed for the $\nu g_{7/2}[404]7/2^+$ bands in the $N = 73$ isotones than in the $N = 75$ ones. The energy gap between the $Z = 73$ Ta and $Z = 75$ Re nuclei exhibits a different behavior. As shown in Fig. 5, instead of a nearly constant energy gap like in the odd-N nuclei mentioned above, an increasing gap with increasing neutron number can be seen in the three pairs of (Ta, Re) isotones with the neutron numbers of 100, 102, and 108.

It is worth mentioning that the accompanying $\pi d_{5/2}[402]5/2^+$ pseudospin partner bands were systematically observed in the odd-Z Ta and Re isotopes, while no bands corresponding to the $\nu d_{5/2}[402]5/2^+$ were observed in the $N = 73$ and 75 isotones of Ba and Ce nuclei. This may be related to the opposite order of the $[404]7/2^+$ and $[402]5/2^+$ Nilsson orbitals at the Fermi level for protons and neutrons. The $N = 74$ gap exists between the $\nu g_{7/2}[404]7/2^+$ and $\nu h_{11/2}[514]9/2^-$ orbitals as mentioned above, while the $\pi d_{5/2}[402]5/2^+$ orbital comes in between the corresponding proton orbitals.

Quite different signature splitting occurs among the $\pi g_{7/2}[404]7/2^+$ and $\nu g_{7/2}[404]7/2^+$ bands. The $\pi g_{7/2}$ bands exhibit little splitting in both Ta and Re isotopes, while relatively large splittings are present in both the N=73 and 75 isotones. In particular, the splitting amplitudes in the N=75 isotones of ^{131}Ba and ^{133}Ce are about 10 times larger than those in the Ta and Re isotopes. The splitting could not be attributed to the configuration mixing with the pseudospin partner $\nu d_{5/2}[402]5/2^+$ orbital, since the mixing, if it exists, is expected to show

no essential difference in the way they act on the valence proton and valence neutron. Additionally, the $\pi d_{5/2}[402]5/2^+$ bands without signature splitting were systematically observed in the odd-A Ta and Re isotopes [49–54].

However, such a significant difference in signature splitting between the $N = 73, 75$ and $Z = 73, 75$ nuclei should reflect differences in the nuclear structure. Since the triaxiality is believed to play a key role in signature splitting, the structure change may be caused by the difference in triaxiality between the various isotopes. In fact, the impact of triaxiality on the rotational structure was investigated in detail for the neutron-rich Re isotopes by Reed *et al.* in Ref. [16], where it was shown that the increasing signature splitting of the $\pi h_{11/2}[514]9/2^-$ bands implies the increasing γ deformation towards the neutron-rich Re isotopes. A similar scenario is expected for the signature splitting in the Ba and Ce nuclei. As shown in Fig. 6, it is interesting to study if the increasing splitting amplitudes in $N = 73$ and $N = 75$ isotones only can be attributed to increasing triaxiality.

C. Theoretical calculations and the Origin of the signature splitting

In the present work, cranked shell model (CSM), quasiparticle-plus-triaxial-rotor (QTR) model, and configuration-constrained potential energy surface (PES) calculations have been performed to get a deeper understanding of the signature splitting systematics. The configuration-constrained PES calculations have been performed within the framework of the macroscopic-microscopic model. The Woods-Saxon type nuclear potential with universal parameters was adopted when solving the single-particle Schrödinger equation (for more details, see Refs. [42–44] and references therein). The results are listed in Table III. In both ^{131}Ba and ^{133}Ce, the CSM calculations for $\gamma = 0°$ at low frequencies ($\hbar\omega \leq 0.3$ MeV) predict no energy splitting for the two signatures of the $\nu g_{7/2}[404]7/2^+$ band. The splitting emerges for $\gamma \sim 10°$ and its amplitude increases with increasing γ values as shown in Fig. 7.

The QTR model [45] is applied to investigate the observed signature staggering in the $g_{7/2}$ bands of ^{131}Ba and ^{133}Ce. The model is based on the Nilsson potential and includes pairing. The γ dependence of the moments of inertia is described with the irrotational-flow model. Ten positive-parity orbitals near the neutron Fermi level are included in the configuration space. The calculations are carried out using the shape parameters listed in Table III, that is $\epsilon_2 = 0.185$, $\gamma = 10°$ and $\epsilon_4 = 0.01$ for ^{133}Ce and $\epsilon_2 = 0.170$, $\gamma = 8°$ and $\epsilon_4 = 0.003$ for ^{131}Ba. Here the ϵ parameterization is used, while in Table III the deformation parameters are given in terms of the Woods-Saxon parameterization. An approximate relation between them is $\epsilon_2 \approx 0.95\beta_2$ (for more details see Refs. [74–76]).

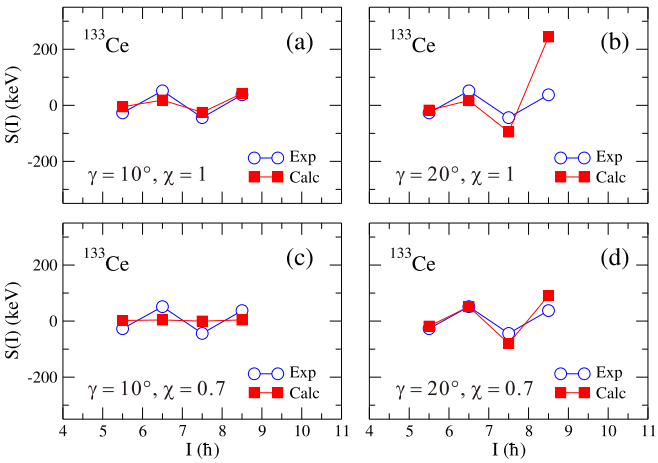

FIG. 8. Experimental and theoretical signature splittings for the $\nu g_{7/2}[404]7/2^+$ band in ^{133}Ce. The calculations are carried out for standard Coriolis interaction ($\chi = 1$) and $\gamma = 10°$ (a) and 20° (b), and for attenuated Coriolis interaction ($\chi = 0.7$) and $\gamma = 10°$ (c) and 20° (d).

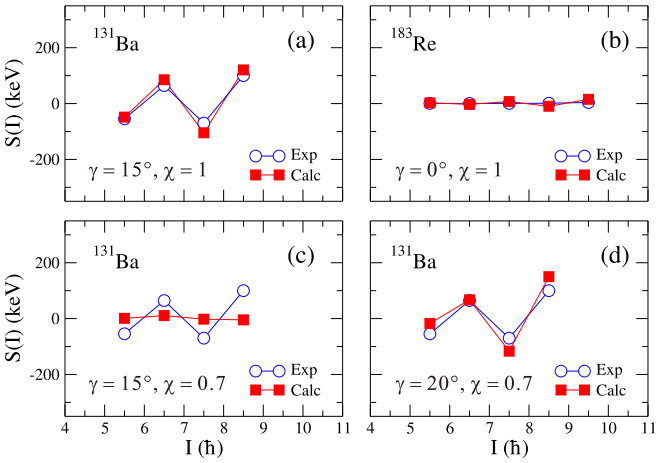

FIG. 9. Experimental and theoretical signature splittings for the $\nu g_{7/2}$ $[404]7/2^+$ band in ^{131}Ba and the $\pi g_{7/2}[404]7/2^+$ band in ^{183}Re. The calculations are carried out for standard Coriolis interaction ($\chi = 1$) and $\gamma = 15°$ (a) and 0° (b), and for attenuated Coriolis interaction ($\chi = 0.7$) and $\gamma = 15°$ (c) and 20° (d).

The calculated excitation energies of the states are in very good agreement with the experimental ones. The signature staggering $S(I)$ is well reproduced with $\gamma = 10°$ for ^{133}Ce, as shown in Fig. 8 (a). For ^{131}Ba the best agreement is obtained for $\gamma = 15°$, see Fig. 9 (a).

The wave functions for the states of the $g_{7/2}$ bands indicate that, in addition to the dominant contribution from the $g_{7/2}$ $[404]7/2^+$ orbital, there are also small contributions from the $s_{1/2}[400]1/2^+$ orbital. Indeed, this orbital is predicted to lie very close to the Fermi surface: it is in fact associated with the ground-state band 3.

It is known that in axially symmetric nuclei bands associated with high-Ω configurations show negligible en-

ergy staggering, because there is a large energy gap that separates them from the $\Omega = 1/2$ orbital of the same sub-shell. An interaction with the $\Omega = 1/2$ orbital is known to generate signature splitting because of Coriolis interaction. For the ^{131}Ba and ^{133}Ce nuclei the $s_{1/2}[400]1/2^+$ orbital happens to have a similar excitation energy to the $g_{7/2}$ $[404]7/2^+$ orbital, and therefore the mixing with the $s_{1/2}[400]1/2^+$ orbital is possible and give rise to signature splitting.

In order to study the impact of the two possible mechanisms that can generate energy staggering, which are the non-axiality of the nuclear shape and the Coriolis interaction, QTR calculations have been carried out as a function of γ. The magnitude and the phase of the staggering was found to remain similar for the entire range of $0^\circ \leq \gamma \leq 15^\circ$ in ^{133}Ce, while for ^{131}Ba the staggering pattern for $\gamma \leq 15^\circ$ was found to have similar magnitude but with a change in phase. However, for both ^{133}Ce and ^{131}Ba nuclei the magnitude of the staggering increases rapidly for $\gamma > 15^\circ$, see for instance Fig. 8 (b). This shows that the triaxiality has a major impact on the energy staggering when the shape corresponds to considerable non-axiality.

To further test the impact of the Coriolis interaction on the staggering for near-axially symmetric shapes, the QTR calculations have been carried out with an attenuation of 70% to the Coriolis interaction ($\chi = 0.7$). The results show no energy staggering for $0^\circ \leq \gamma \leq 15^\circ$, (see Figs. 8 (c) and 9 (c)), but a significant staggering for $\gamma > 15^\circ$, (see Figs. 8 (d) and 9 (d)).

In addition, QTR calculations have been carried out for the $\pi g_{7/2}$ band in the $Z = 75$ ^{183}Re nucleus. While there are many similarities between the $N = 75$ and $Z = 75$ nuclei, there also exists an important difference, that for protons the $s_{1/2}$ sub-shell lies at higher excitation energy with respect to the $g_{7/2}$ sub-shell. Thus, while for $N = 75$ the excitation energies of the $\nu s_{1/2}[400]1/2^+$ and $\nu g_{7/2}[404]7/2^+$ orbitals are similar, the excitation energies of the $\pi s_{1/2}[400]1/2^+$ and $\pi g_{7/2}[404]7/2^+$ proton orbitals are different. The QTR calculations for ^{183}Re reproduce well the excitation energies of the $\pi g_{7/2}$ band assuming $\gamma = 0^\circ$ and standard strength of the Coriolis interaction ($\chi = 1$). They predict no signature splitting, see Fig. 9 (b), in agreement with the experimental observations.

The QTR calculations suggest that the $g_{7/2}$ bands in the $N = 75$ isotopes ^{133}Ce and ^{131}Ba are generated by two competing mechanisms, the Coriolis interaction caused by the mixture with the close-in-energy $s_{1/2}$ orbital, and the non-axiality of the nuclear shape.

In the lighter Ba, Ce, and Nd isotopes, instead of the $\nu g_{7/2}[404]7/2^+$ bands, the $\nu d_{5/2}[402]5/2^+$ bands were systematically observed with very small or no energy splitting at low spin (see Fig. 10). This can be also attributed to negligible mixing of the $\nu s[400]1/2^+$ orbital with the $\nu d_{5/2}[402]5/2^+$ orbital which lies further away from the low-j ones.

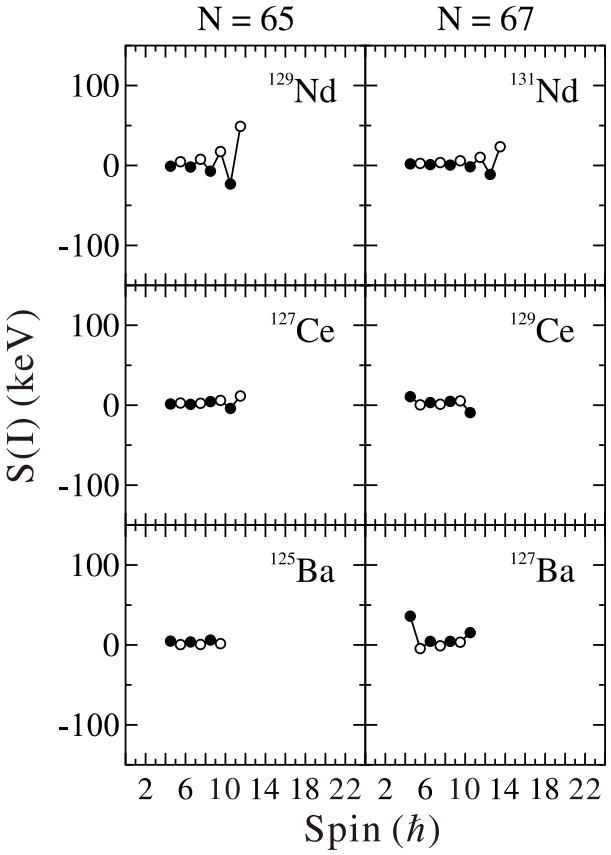

FIG. 10. Similar to Fig. 6, but for the $\nu d_{5/2}[402]5/2^+$ bands in the $N = 65$ and 67 isotones. Data are taken from [77] for ^{125}Ba, [78] for ^{127}Ce, [79] for ^{129}Nd, [80] for ^{127}Ba, [78] for ^{129}Ce, and [81] for ^{131}Nd.

IV. SUMMARY

Excited states in ^{131}Ba and ^{133}Ce have been investigated via standard in-beam γ-spectroscopy experiments using the ^{122}Sn(^{13}C,4n)^{131}Ba and ^{125}Te(^{12}C,4n)^{133}Ce reactions, respectively. Besides the previously reported one-quasiparticle bands built on the $I^\pi = 9/2^-$ state and the $I^\pi = 1/2^+$ ground state, new bands based on $I^\pi = 7/2^+$ have been identified in both nuclei. The bands exhibit strong-coupling characteristics and have been assigned to the $\nu g_{7/2}[404]7/2^+$ configuration. By comparison with the corresponding proton $\pi[404]7/2^+$ bands in the odd-A Ta and Re isotopes, relatively large signature splittings have been observed in the neutron $\nu[404]7/2^+$ bands of the $N = 73, 75$ nuclei. In particular, the splitting amplitudes in the $N = 75$ isotones of ^{131}Ba and ^{133}Ce are about 10 times larger than those in the odd-Z nuclei.

The CSM calculations show that the splitting amplitudes of the bands increase with the increasing triaxial parameter γ. For ^{131}Ba and ^{133}Ce, the splitting amplitudes are consistent with the values predicted by the QTR model with triaxial deformation parameters

TABLE III. Calculated excitation energies $E_{\rm cal}$ (keV) and shapes of the possible one-quasiparticle states in ^{131}Ba and ^{133}Ce, compared with the experimentally determined values $E_{\rm exp}$.

I^π	$E_{\rm exp}$	$E_{\rm cal}$	Configuration	β_2	γ°	β_4
^{131}Ba						
$9/2^-$	188.0	0	$\nu[514]9/2^-$	0.178	20.6	−0.010
$1/2^+$	0	35	$\nu[400]1/2^+$	0.172	20.9	−0.006
$1/2^+$		609	$\nu[411]1/2^+$	0.187	28.5	0.006
$3/2^+$		428	$\nu[402]3/2^+$	0.160	−0.1	0.000
$7/2^+$	525.3	420	$\nu[404]7/2^+$	0.180	9.1	−0.014
$5/2^+$		1005	$\nu[402]5/2^+$	0.177	11.8	−0.013
^{133}Ce						
$9/2^-$	37.2	0	$\nu[514]9/2^-$	0.193	21.1	−0.018
$1/2^+$	0	125	$\nu[400]1/2^+$	0.185	20.3	−0.013
$1/2^+$		649	$\nu[411]1/2^+$	0.193	27.7	−0.003
$3/2^+$		315	$\nu[402]3/2^+$	0.181	−1.0	−0.020
$7/2^+$	340.3	371	$\nu[404]7/2^+$	0.195	−10.5	−0.023
$5/2^+$		950	$\nu[402]5/2^+$	0.192	13.0	−0.023

$\gamma = 15^\circ$ and $\gamma = 10^\circ$, respectively. However, QTR calculations predict that not only the triaxiality but also the Coriolis interaction generated by the mixing with low-j orbitals are responsible for the observed signature splitting. The present work can trigger more comprehensive theoretical investigations on this topic aiming to a full understanding of the mechanisms causing signature splitting of the $\Omega = j$ configurations.

V. ACKNOWLEDGEMENT

This research is supported by the National Natural Science Foundation of China (Grants No. U2032144, No. 11975209, No. U1932137, No. U1732139, No. U1832134, No. 11805289, No. 11775274, and No. 11575255), by the Minister of Europe and Foreign Affairs, Partnership Hubert Curien, Project Cai Yuan-Pei 2018, Grant No. 41458XH, by the Natural Sciences and Engineering Research Council of Canada, by the National Research, Development and Innovation Fund of Hungary with Project No. K128947, by the European Regional Development Fund (Contract No. GINOP-2.3.3-15-2016-00034), by the National Research, Development and Innovation Office NKFIH (Contract No. PD 124717), by the Polish National Science Centre (NCN) (Grants No. 2017/25/B/ST2/01569 and 2020/39/D/ST2/00466), by the National Research Foundation of South Africa (Grants No. 116666 and No. 109134), by the French Ministry of Foreign Affairs and the Ministry of Higher Education and Research, France (PHC PROTEA Grant No. 42417SE), and by the U.S. Department of Energy, Office of Science, Office of Nuclear Physics (Contract No. DE-AC02-06CH11357).

[1] F. S. Stephens, Rev. Mod. Phys. **47**, 43 (1975).
[2] D. Bucurescuand N. V. Zamfir, Phys. Rev. C **95**, 014329 (2017).
[3] C. Y. Wu, H. Hua, D. Cline, A. B. Hayes, R. Teng, R. M. Clark, P. Fallon, A. Goergen, A. O. Macchiavelli, and K. Vetter, Phys. Rev. C **70**, 064312 (2004).
[4] J. K. Hwang, A. V. Ramayya, J. H. Hamilton, D. Fong, C. J. Beyer, P. M. Gore, Y. X. Luo, J. O. Rasmussen, S. C. Wu, I. Y. Lee, C. M. Folden, P. Fallon, P. Zielinski, K. E. Gregorich, A. O. Macchiavelli, M. A. Stoyer, S. J. Asztalos, T. N. Ginter, S. J. Zhu, J. D. Cole, G. M. Ter Akopian, Y. T. Oganessian, and R. Donangelo, Phys. Rev. C **67**, 054304 (2003).
[5] Y. Liang, D. B. Fossan, J. R. Hughes, D. R. LaFosse, T. Lauritsen, R. Ma, E. S. Paul, P. Vaska, M. P. Waring, and N. Xu, Phys. Rev. C **45**, 1041 (1992).
[6] S. Y. Wang, T. Komatsubara, Y. J. Ma, K. Furuno, Y. H. Zhang, Y. Z. Liu, T. Hayakawa, J. Mukai, Y. Iwata, T. Morikawa, G. B. Hagemann, G. Sletten, J. Nyberg, D. Jerrestam, H. J. Jensen, J. Espino, J. Gascon, N. Gjrup, B. Cederwall, and P. O. Tjm, J. Phys. G: Nucl. Part. Phys. **32**, 283 (2006).
[7] F. Liden, B. Caderwall, P. Ahonen, D. W. Banes, B. Fant, J. Gascn, L. Hildingsson, A. Johnson, S. Juutinen, A. Kirwan, D. Love, S. Mitarai, J. Mukai, A. Nelson, J. Nyberg, J. Simpson, and R. Wyss, Nucl. Phys. A **550**, 365 (1992).
[8] J. Sun, Y.-J. Ma, T. Komatsubara, K. Furuno, Y.-H. Zhang, W.-P. Zhou, S.-Y. Wang, X.-Y. Hu, H. Guo, J.-Q. Wang, and Y.-Z. Liu, Phys. Rev. C **93**, 064301 (2016).
[9] Y. Liang, R. Ma, E. S. Paul, N. Xu, D. B. Fossan, and R. A. Wyss, Phys. Rev. C **42**, 890 (1990).

[10] S. T. Wang, X. H. Zhou, Y. H. Zhang, Y. Zheng, M. L. Liu, L. Chen, N. T. Zhang, W. Hua, S. Guo, Y. H. Qiang, G. S. Li, B. Ding, Y. Shi, and F. R. Xu, Phys. Rev. C **84**, 017303 (2011).

[11] A. Jungclaus, B. Binder, A. Dietrich, T. Härtlein, H. Bauer, C. Gund, D. Pansegrau, D. Schwalm, D. Bazzacco, E. Farnea, S. Lunardi, C. Rossi-Alvarez, C. Ur, G. de Angelis, A. Gadea, D. R. Napoli, X. R. Zhou, and Y. Sun, Phys. Rev. C **67**, 034302 (2003).

[12] T. Shizuma, T. Ishii, H. Makii, T. Hayakawa, M. Matsuda, S. Shigematsu, E. Ideguchi, Y. Zheng, M. Liu, T. Morikawa, and M. Oi, Phys. Rev. C **77**, 047303 (2008).

[13] V. Bondarenko, A. V. Afanasjev, T. von Egidy, L. Simonova, J. Berzinš, I. Kuvaga, W. Schauer, J. Ott, P. Prokofjevs, R. Georgii, M. Kessler, T. Körbitz, and W. Schott, Nucl. Phys. A **619**, 1 (1997).

[14] J. Meyer-Ter-Vehn, Nucl. Phys. A **249**, 111 (1975).

[15] J. Meyer-Ter-Vehn, Nucl. Phys. A **249**, 141 (1975).

[16] M. W. Reed, G. J. Lane, G. D. Dracoulis, F. G. Kondev, M. P. Carpenter, P. Chowdhury, S. S. Hota, R. O. Hughes, R. V. F. Janssens, T. Lauritsen, C. J. Lister, N. Palalani, D. Seweryniak, H. Watanabe, S. Zhu, W. G. Jiang, and F. R. Xu, Phys. Lett. B **752**, 311 (2016).

[17] P. Möller, R. Bengtsson, B. G. Carlsson, P. Olivius, T. Ichikawa, H. Sagawa, and A. Iwamoto, At. Data Nucl. Data Tables **94**, 758 (2008).

[18] S. Frauendorfand M. Jie, Nucl. Phys. A **617**, 131 (1997).

[19] K. Starosta, T. Koike, C. J. Chiara, D. B. Fossan, D. R. LaFosse, A. A. Hecht, C. W. Beausang, M. A. Caprio, J. R. Cooper, R. Krucken, J. R. Novak, N. V. Zamfir, K. E. Zyromski, D. J. Hartley, D. L. Balabanski, J. Y. Zhang, S. Frauendorf, and V. I. Dimitrov, Phys. Rev. Lett. **86**, 971 (2001).

[20] E. S. Paul, R. Ma, C. W. Beausang, S. A. Forbes, D. B. Fossan, J. Gizon, J. R. Hughes, Y. Liang, S. M. Mullins, P. J. Nolan, W. F. Piel, R. J. Poynter, P. H. Regan, R. Wadsworth, and N. Xu, J. Phys. G: Nucl. Part. Phys. **17**, 605 (1991).

[21] A. Granderath, P. F. Mantica, R. Bengtsson, R. Wyss, P. vonBrentano, A. Gelberg, and F. Seiffert, Nucl. Phys. A **597**, 427 (1996).

[22] T. Koike, K. Starosta, C. J. Chiara, D. B. Fossan, and D. R. LaFosse, Phys. Rev. C **67**, 044319 (2003).

[23] R. Ma, Y. Liang, E. S. Paul, N. Xu, D. B. Fossan, L. Hildingsson, and R. A. Wyss, Phys. Rev. C **41**, 717 (1990).

[24] R. Ma, E. S. Paul, C. W. Beausang, S. Shi, N. Xu, and D. B. Fossan, Phys. Rev. C **36**, 2322 (1987).

[25] S. Guo, C. M. Petrache, D. Mengoni, Y. H. Qiang, Y. P. Wang, Y. Y. Wang, J. Meng, Y. K. Wang, S. Q. Zhang, P. W. Zhao, A. Astier, J. G. Wang, H. L. Fan, E. Dupont, B. F. Lv, D. Bazzacco, A. Boso, A. Goasduff, F. Recchia, D. Testov, F. Galtarossa, G. Jaworski, D. R. Napoli, S. Riccetto, M. Siciliano, J. J. Valiente-Dobon, M. L. Liu, G. S. Li, X. H. Zhou, Y. H. Zhang, C. Andreoiu, F. H. Garcia, K. Ortner, K. Whitmore, A. Ataç-Nyberg, T. Bäck, B. Cederwall, E. A. Lawrie, I. Kuti, D. Sohler, T. Marchlewski, J. Srebrny, and A. Tucholski, Phys. Lett. B **807**, 135572 (2020).

[26] A. D. Ayangeakaa, U. Garg, C. M. Petrache, S. Guo, P. W. Zhao, J. T. Matta, B. K. Nayak, D. Patel, R. V. F. Janssens, M. P. Carpenter, C. J. Chiara, F. G. Kondev, T. Lauritsen, D. Seweryniak, S. Zhu, S. S. Ghugre, and R. Palit, Phys. Rev. C **93**, 054317 (2016).

[27] C. B. Creager, C. W. Kocher, and A. C. G. Mitchell, Nucl.Phys. **14**, 578 (1960).

[28] B. Harmatzand T. H. Handley, Nucl. Phys. A **191**, 497 (1972).

[29] D. J. Horen, W. H. Kelly, and L. Yaffe, Phys. Rev. **129**, 1712 (1963).

[30] D. von Ehrenstein, G. C. Morrison, J. A. Nolen, and N. Williams, Phys. Rev. C **1**, 2066 (1970).

[31] G. Suliman, D. Bucurescu, R. Hertenberger, H. F. Wirth, T. Faestermann, R. Krücken, T. Behrens, V. Bildstein, K. Eppinger, C. Hinke, M. Mahgoub, P. Meierbeck, M. Reithner, S. Schwertel, and N. Chauvin, Eur. Phys. J. A **46**, 187 (2010).

[32] J. Gizon, A. Gizon, and D. J. Horen, Nucl. Phys. A **252**, 509 (1975).

[33] N. Kaur, A. Kumar, G. Mukherjee, A. Singh, S. Kumar, R. Kaur, V. Singh, B. R. Behera, K. P. Singh, G. Singh, H. P. Sharma, S. Kumar, M. Kumar Raju, P. V. Madhusudhan Rao, S. Muralithar, R. P. Singh, R. Kumar, N. Madhvan, and R. K. Bhowmik, Eur. Phys. J. A **50**, 5 (2014).

[34] M. S. Rapaport, D. Bucurescu, C. F. Liang, and P. Paris, Phys. Rev. C **42**, 1959 (1990).

[35] J. Gizon, A. Gizon, M. R. Maier, R. M. Diamond, and F. S. Stephens, Nucl. Phys. A **222**, 557 (1974).

[36] A. D. Ayangeakaa, U. Garg, M. D. Anthony, S. Frauendorf, J. T. Matta, B. K. Nayak, D. Patel, Q. B. Chen, S. Q. Zhang, P. W. Zhao, B. Qi, J. Meng, R. V. Janssens, M. P. Carpenter, C. J. Chiara, F. G. Kondev, T. Lauritsen, D. Seweryniak, S. Zhu, S. S. Ghugre, and R. Palit, Phys. Rev. Lett. **110**, 172504 (2013).

[37] K. Hauschild, R. Wadsworth, R. M. Clark, I. M. Hibbert, P. Fallon, A. O. Macchiavelli, D. B. Fossan, H. Schnare, I. Thorslund, P. J. Nolan, A. T. Semple, and L. Walker, Phys. Rev. C **54**, 613 (1996).

[38] E. S. Paul, R. Ma, C. W. Beausang, S. A. Forbes, D. B. Fossan, J. Gizon, J. R. Hughes, Y. Liang, S. M. Mullins, P. J. Nolan, W. F. Piel, R. J. Poynter, P. H. Regan, R. Wadsworth, and N. Xu, J. Phys. G: Nucl. Part. Phys. **17**, 605 (1991).

[39] L. G. R. Emediato, M. N. Rao, N. H. Medina, W. A. Seale, S. Botelho, R. V. Ribas, J. R. B. Oliveira, E. W. Cybulska, F. R. Espinoza-Quiñones, V. Guimarães, M. A. Rizzutto, and J. C. Acquadro, Phys. Rev. C **55**, 2105 (1997).

[40] K. Hauschild, R. Wadsworth, R. M. Clark, P. Fallon, D. B. Fossan, I. M. Hibbert, A. O. Macchiavelli, P. J. Nolan, H. Schnare, A. T. Semple, I. Thorslund, L. Walker, W. Satula, and R. Wyss, Phys. Lett. B **353**, 438 (1995).

[41] A. T. Semple, P. J. Nolan, C. W. Beausang, S. A. Forbes, E. S. Paul, J. N. Wilson, R. Wadsworth, K. Hauschild, I. M. Hibbert, R. M. Clark, J. Gizon, A. Gizon, D. Santos, and J. Simpson, Phys. Rev. Lett. **76**, 3671 (1996).

[42] F. R. Xu, P. M. Walker, J. A. Sheikh, and R. Wyss, Phys. Lett. B **435**, 257 (1998).

[43] H. L. Liu, F. R. Xu, S. W. Xu, R. Wyss, and P. M. Walker, Phys. Rev. C **76**, 034313 (2007).

[44] Y. Shi, P. M. Walker, and F. R. Xu, Phys. Rev. C **85**, 027307 (2012).

[45] P. B. Semmesand I. Ragnarsson, in *Proceedings of the International Conference on High-Spin Physics and Gamma-Soft Nuclei, Pittsburg,* edited by J. X. Saladin, R. A. Sorenson, and C. M. Vincent (World Scientific,

Singapore, 1991), p. 500; in *Future Directions in Nuclear Physics with 4π Gamma Detection Systems of the New Generation*, edited by J. Dudek and B. Haas,, AIP Conf. Proc. No. 259 (AIP, Woodbury, NY, 1992), p. 566.

[46] A. P. Byrne, K. Schiffer, G. D. Dracoulis, B. Fabricius, T. Kibédi, A. E. Stuchbery, and K. P. Lieb, Nucl. Phys. A **548**, 131 (1992).

[47] M. Palacz, Z. Sujkowski, J. Nyberg, J. Bacelar, J. Jongman, W. Urban, W. Hesselink, J. Nasser, A. Plompen, and R. Wyss, Z. Phys. A **338**, 467 (1991).

[48] D. Bazzacco, F. Brandolini, G. Falconi, S. Lunardi, N. H. Medina, P. Pavan, C. Rossi Alvarez, G. de Angelis, D. De Acuna, M. De Poli, D. R. Napoli, J. Rico, D. Bucurescu, M. Ionescu-Bujor, and C. A. Ur, Phys. Rev. C **58**, 2002 (1998).

[49] H. Q. Jin, L. L. Riedinger, C. H. Yu, W. Nazarewicz, R. Wyss, J. Y. Zhang, C. Baktash, J. D. Garrett, N. R. Johnson, I. Y. Lee, and F. K. McGowan, Phys. Lett. B **277**, 387 (1992).

[50] R. A. Bark, G. B. Hagemann, B. Herskind, H. J. Jensen, W. Korten, J. Wrzesinski, H. Carlsson, M. Bergström, A. Brockstedt, A. Nordlund, H. Ryde, P. Bosetti, S. Leoni, F. Ingebretsen, and P. O. Tjøm, Nucl. Phys. A **591**, 265 (1995).

[51] C. S. Purry, P. M. Walker, G. D. Dracoulis, S. Bayer, A. P. Byrne, T. Kibédi, F. G. Kondev, C. J. Pearson, J. A. Sheikh, and F. R. Xu, Nucl. Phys. A **672**, 54 (2000).

[52] H. Carlsson, R. A. Bark, L. P. Ekström, A. Nordlund, H. Ryde, C. B. Hagemann, S. J. Freeman, H. J. Jensen, T. Lönnroth, M. J. Piiparinen, H. Schnack-Petersen, F. Ingebretsen, and P. O. Tjøm, Nucl. Phys. A **592**, 89 (1995).

[53] S.-X. Wen, H. Zheng, S.-G. Li, G.-S. Li, G.-J. Yuan, P.-F. Hua, P.-K. Weng, L.-K. Zhang, P.-S. Yu, C.-X. Yang, H.-B. Sun, Y.-B. Liu, Y.-Z. Liu, Y. Sun, and D. H. Feng, Phys. Rev. C **54**, 1015 (1996).

[54] T. R. Saitoh, N. Hashimoto, G. Sletten, R. A. Bark, S. Törmänen, M. Bergström, K. Furuno, K. Furutaka, G. B. Hagemann, T. Hayakawa, T. Komatsubara, A. Maj, S. Mitarai, M. Oshima, J. Sampson, T. Shizuma, and P. G. Varmette, Eur. Phys. J. A **3**, 197 (1998).

[55] A. Goasduff *et al.*, unpublished.

[56] D. Testov, D. Mengoni, A. Goasduff, A. Gadea, R. Isocrate, P. R. John, G. de Angelis, D. Bazzacco, C. Boiano, A. Boso, P. Cocconi, J. A. Dueñas, F. J. Egea Canet, L. Grassi, K. Hadyńska-Klek, G. Jaworski, S. Lunardi, R. Menegazzo, D. R. Napoli, F. Recchia, M. Siciliano, and J. J. Valiente-Dobón, Eur. Phys. J. A **55**, 47 (2019).

[57] O. Skeppstedt, H. A. Roth, L. Lindström, R. Wadsworth, I. Hibbert, N. Kelsall, D. Jenkins, H. Grawe, M. Górska, M. Moszyóski, Z. Sujkowski, D. Wolski, M. Kapusta, M. Hellström, S. Kalogeropoulos, D. Oner, A. Johnson, J. Cederkäll, W. Klamra, J. Nyberg, M. Weiszflog, J. Kay, R. Griffiths, J. Garces Narro, C. Pearson, and J. Eberth, Nucl. Instrum. Methods Phys. Res., Sect. A **421**, 531 (1999).

[58] J. Ljungvall, M. Palacz, and J. Nyberg, Nucl. Instrum. Methods Phys. Res., Sect. A **528**, 741 (2004).

[59] L. Berti, M. Biasotto, S. Fantinel, A. A. Gozzelino, M. Gulmini, and N. Toniolo, LNL INFN Annual Report , p.93 (2014(unpublished)).

[60] D. C. Radford, Nucl. Instrum. Methods Phys. Res., Sect. A **361**, 297 (1995).

[61] D. Bazzacco and N. Mărginean (private communication).

[62] A. Krämer-Flecken, T. Morek, R. M. Lieder, W. Gast, G. Hebbinghaus, H. M. Jäger, and W. Urban, Nucl. Instrum. Methods Phys. Res., Sect. A **275**, 333 (1989).

[63] S. Guo, C. M. Petrache, D. Mengoni, Y. X. Liu, Q. B. Chen, Y. H. Qiang, A. Astier, E. Dupont, K. K. Zheng, J. G. Wang, B. Ding, B. F. Lv, M. L. Liu, Y. D. Fang, X. H. Zhou, D. Bazzacco, A. Boso, A. Goasduff, F. Recchia, D. Testov, F. Galtarossa, G. Jaworski, D. R. Napoli, S. Riccetto, M. Siciliano, J. J. Valiente-Dobon, C. Andreoiu, F. H. Garcia, K. Ortner, K. Whitmore, B. Cederwall, E. A. Lawrie, I. Kuti, D. Sohler, T. Marchlewski, J. Srebrny, and A. Tucholski, Phys. Rev. C **102**, 044320 (2020).

[64] Y. H. Qiang, C. M. Petrache, S. Guo, P. M. Walker, D. Mengoni, Q. B. Chen, B. F. Lv, A. Astier, E. Dupont, M. L. Liu, X. H. Zhou, J. G. Wang, D. Bazzacco, A. Boso, A. Goasduff, F. Recchia, D. Testov, F. Galtarossa, G. Jaworski, D. R. Napoli, S. Riccetto, M. Siciliano, J. J. Valiente-Dobon, C. Andreoiu, F. H. Garcia, K. Ortner, K. Whitmore, B. Cederwall, E. A. Lawrie, I. Kuti, D. Sohler, T. Marchlewski, J. Srebrny, A. Tucholski, A. C. Dai, and F. R. Xu, Phys. Rev. C **99**, 014307 (2019).

[65] R. T. Newman *et al.*, Balkan Phys. Lett., Special Issue **182** (1998).

[66] J. Sharpey-Schafer, Nucl. Phys. News **14**, 5 (2004).

[67] T. Shizuma, T. Ishii, H. Makii, T. Hayakawa, S. Shigematsu, M. Matsuda, E. Ideguchi, Y. Zheng, M. Liu, and T. Morikawa, Eur. Phys. J. A **34**, 1 (2007).

[68] T. Shizuma, T. Ishii, H. Makii, T. Hayakawa, and M. Matsuda, Eur. Phys. J. A **39**, 263 (2009).

[69] F. G. Kondev, G. D. Dracoulis, A. P. Byrne, T. Kibédi, and S. Bayer, Nucl. Phys. A **617**, 91 (1997).

[70] M. Dasgupta, G. D. Dracoulis, P. M. Walker, A. P. Byrne, T. Kibédi, F. G. Kondev, G. J. Lane, and P. H. Regan, Phys. Rev. C **61**, 044321 (2000).

[71] D. J. Hartley, W. H. Mohr, J. R. Vanhoy, M. A. Riley, A. Aguilar, C. Teal, R. V. F. Janssens, M. P. Carpenter, A. A. Hecht, T. Lauritsen, E. F. Moore, S. Zhu, F. G. Kondev, M. K. Djongolov, M. Danchev, L. L. Riedinger, G. B. Hagemann, G. Sletten, P. Chowdhury, S. K. Tandel, W. C. Ma, and S. W. Ødegärd, Phys. Rev. C **72**, 064325 (2005).

[72] D. J. Hartley, W. H. Mohr, J. R. Vanhoy, M. A. Riley, A. Aguilar, C. Teal, R. V. F. Janssens, M. P. Carpenter, A. A. Hecht, T. Lauritsen, E. F. Moore, S. Zhu, F. G. Kondev, M. K. Djongolov, M. Danchev, L. L. Riedinger, G. B. Hagemann, G. Sletten, P. Chowdhury, S. K. Tandel, W. C. Ma, and S. W. Ødegärd, Phys. Rev. C **74**, 054314 (2006).

[73] D. J. Hartley, R. V. F. Janssens, L. L. Riedinger, M. A. Riley, X. Wang, A. Aguilar, M. P. Carpenter, C. J. Chiara, P. Chowdhury, I. G. Darby, U. Garg, Q. A. Ijaz, F. G. Kondev, S. Lakshmi, T. Lauritsen, A. Ludington, W. C. Ma, E. A. McCutchan, S. Mukhopadhyay, R. Pifer, E. P. Seyfried, U. Shirwadkar, I. Stefanescu, S. K. Tandel, J. R. Vanhoy, S. Zhu, and S. Frauendorf, Phys. Rev. C **83**, 064307 (2011).

[74] P. Möller, A. J. Sierk, T. Ichikawa, and H. Sagawa, At. Data Nucl. Data Tables **109-110**, 1 (2016).

[75] R. Bengtsson, J. Dudek, W. Nazarewicz, and P. Olanders, Phys. Scr. **39**, 196 (1989).

[76] Y. R. Shimizu, T. Shoji, and M. Matsuzaki, Phys. Rev. C **77**, 024319 (2008).

[77] P. Mason, G. Benzoni, A. Bracco, F. Camera, B. Million, O. Wieland, S. Leoni, A. K. Singh, A. Al-Khatib, H. Hübel, P. Bringel, A. Bürger, A. Neusser, G. Schönwasser, B. M. Nyakó, J. Timár, A. Algora, Z. Dombrádi, J. Gál, G. Kalinka, J. Molnár, D. Sohler, L. Zolnai, K. Juhász, G. B. Hagemann, C. R. Hansen, B. Herskind, G. Sletten, M. Kmiecik, A. Maj, J. Styczen, K. Zuber, F. Azaiez, K. Hauschild, A. Korichi, A. Lopez-Martens, J. Roccaz, S. Siem, F. Hannachi, J. N. Scheurer, P. Bednarczyk, T. Byrski, D. Curien, O. Dorvaux, G. Duchêne, B. Gall, F. Khalfallah, I. Piqueras, J. Robin, S. B. Patel, O. A. Evans, G. Rainovski, C. M. Petrache, D. Petrache, G. L. Rana, R. Moro, G. D. Angelis, P. Falon, I. Y. Lee, J. C. Lisle, B. Cederwall, K. Lagergen, R. M. Lieder, E. Podsvirova, W. Gast, H. Jäger, N. Redon, and A. Görgen, Phys. Rev. C **72**, 064315 (2005).

[78] E. S. Paul, J. P. Revill, M. Mustafa, S. V. Rigby, A. J. Boston, C. Foin, J. Genevey, A. Gizon, J. Gizon, I. M. Hibbert, D. T. Joss, P. J. Nolan, B. M. Nyakó, N. J. OBrien, C. M. Parry, A. T. Semple, S. L. Shepherd, J. Timár, R. Wadsworth, and L. Zolnai, Phys. Rev. C **80**, 054312 (2009).

[79] O. Zeidan, D. J. Hartley, L. L. Riedinger, M. Danchev, W. Reviol, W. D. Weintraub, J.-y. Zhang, A. Galindo-Uribarri, C. J. Gross, S. D. Paul, C. Baktash, M. Lipoglavsek, D. C. Radford, C. H. Yu, D. G. Sarantites, M. Devlin, M. P. Carpenter, R. V. F. Janssens, D. Seweryniak, and E. Padilla, Phys. Rev. C **65**, 024303 (2002).

[80] A. Dewald, A. Schmidt, G. Alexius, O. Vogel, R. S. Chakrawarthy, D. Bazzacco, P. von Brentano, A. Gizon, J. Gizon, S. Lunardi, D. R. Napoli, P. Pavan, C. Rossi Alvarez, and I. Wiedenhver, Eur. Phys. J. A **3**, 103 (1998).

[81] D. J. Hartley, W. Reviol, L. L. Riedinger, D. L. Balabanski, H. Q. Jin, B. H. Smith, O. Zeidan, J.-y. Zhang, A. Galindo-Uribarri, D. G. Sarantites, D. R. LaFosse, J. N. Wilson, and S. M. Mullins, Phys. Rev. C **61**, 044328 (2000).